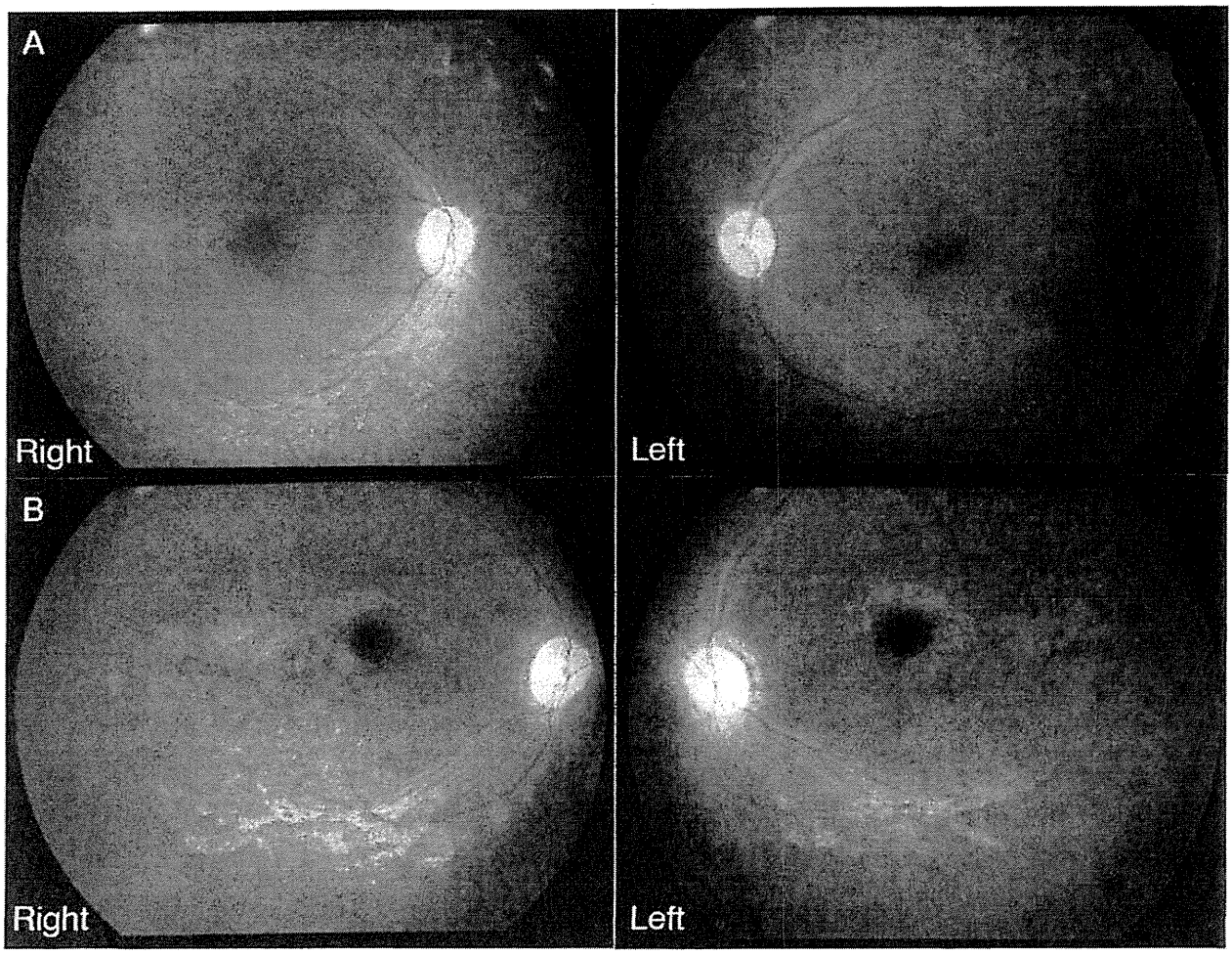

Figure 4. Fundus photographs of patients II-1 and II-2. **A** and **B**: Fundus photographs of patient II-1 at the age of 14 years (**A**) and patient II-2 at the age of 8 years (**B**) show retinal degeneration with attenuated vessels in the posterior poles of both eyes.

combined, photopic, or 30-Hz flicker responses in either eye (Figure 2). GP analysis at the age of 11 years showed markedly constricted visual fields in V-4e and I-4e isopters of both eyes (Figure 3A). The fundus photographs at the age of 14 years showed retinal degeneration with attenuated vessels from the arcade to the periphery in both eyes (Figure 4A). GP analysis at the age of 16 years showed more marked constricted visual fields of V-4e and I-4e isopters in both eyes than those observed at the age of 11 years (Figure 3B); a similar analysis at the age of 22 years showed a small visual field of V-4e isopter in the right eye and no visual field in the left eye (Figure 3C). TD-OCT at the age of 22 years showed total macular thinning in both eyes (Figure 5A). At the age of 29 years, his BCVA was light perception (LP) in the right eye and no light perception in the left eye. Intraocular pressure in each eye was within the normal range. He had severe cortical and subcapsular cataracts in the right (Figure 6) and left eyes, and the fundi were not visible due to these cataracts.

Ophthalmologic findings for patient II-2: Patient II-2, the younger of the two brothers, visited our hospital at the age of 2 years and 6 months with the main complaint of poor visual acuity and photophobia. At the age of 3 years, his BCVA was 0.01 (+1.50 dpt) in the right eye and 0.01 (+1.50 dpt) in the left eye. Fundus examination showed retinal degeneration with slight attenuation of peripheral vessels. At the age of 4 years, he failed the Ishihara test. At the age of 6 years, the panel D-15 test showed irregular arrangements along no particular axis, and the GP could not be measured well because of low visual acuity and nystagmus. The ERG at the age of 7 years showed no rod, standard combined, photopic, or 30-Hz flicker responses in either eye (Figure 2). The fundus examination at

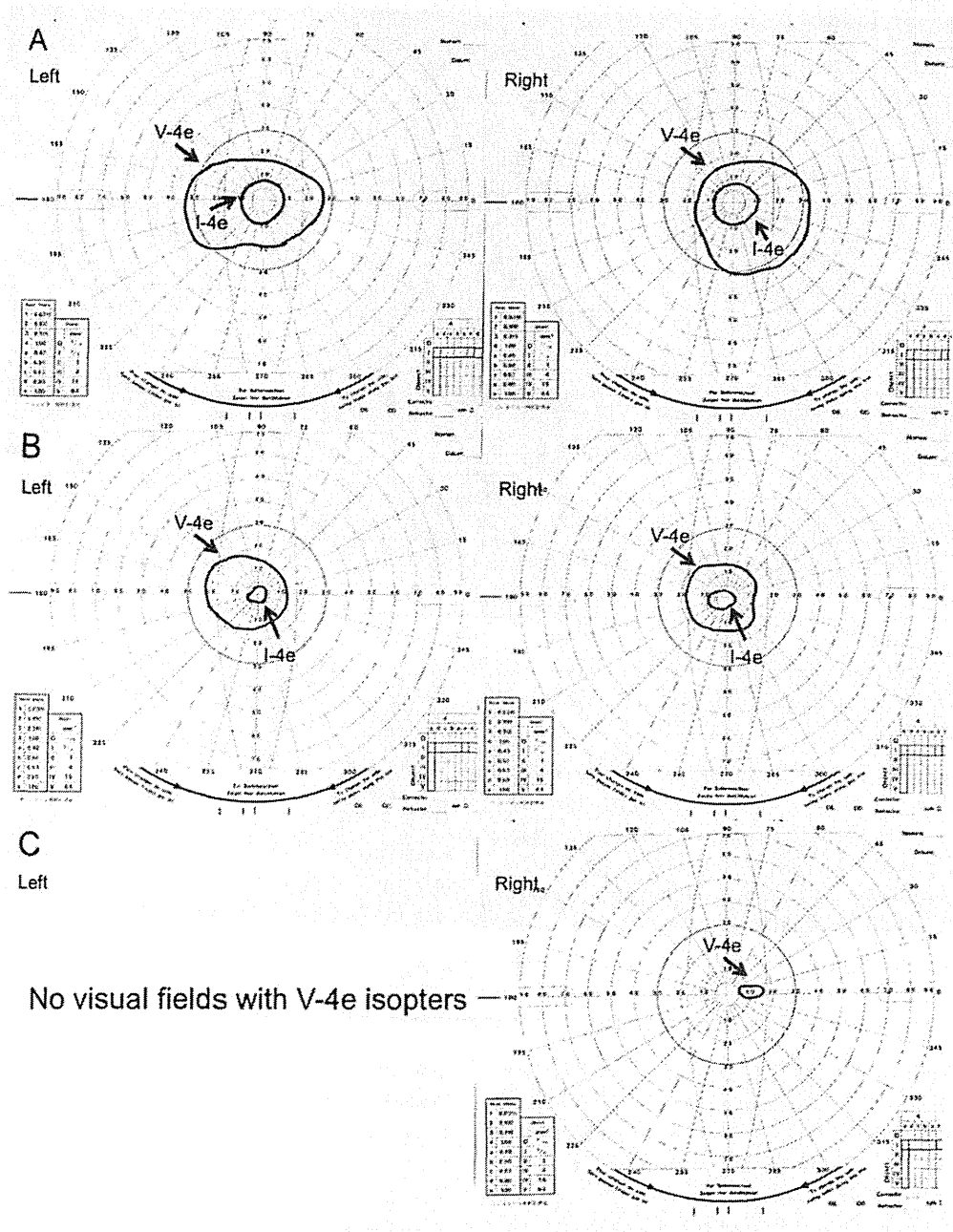

Figure 3. Visual fields assayed by Goldmann perimetry in patient II-1. A–C: Visual fields at the age of 11 years (**A**), at the age of 16 years (**B**), and at the age of 22 years (**C**). Markedly constricted visual fields (V-4e and I-4e isopters) are observed in both eyes, and the visual fields become constricted as the patient ages.

RESULTS

Ophthalmologic findings for patient II-1: Patient II-1, the elder of the two brothers, was referred to our hospital at the age of 7 years and 4 months for the assessment of poor visual acuity from infancy. His BCVA was 0.04 (with +2.00 diopter [dpt], cylinder [cyl] –1.00 dpt axis [Ax] 180°) in the right eye and 0.06 (with +2.00 dpt, cyl –1.00 dpt Ax 180°) in the left eye. Fundus examination showed slight retinal degeneration in both eyes. At the age of 9 years, the patient recognized only the first plate in the Ishihara test for color vision, the panel D-15 test for color vision showed irregular arrangements along no particular axis, and the ERG showed no standard

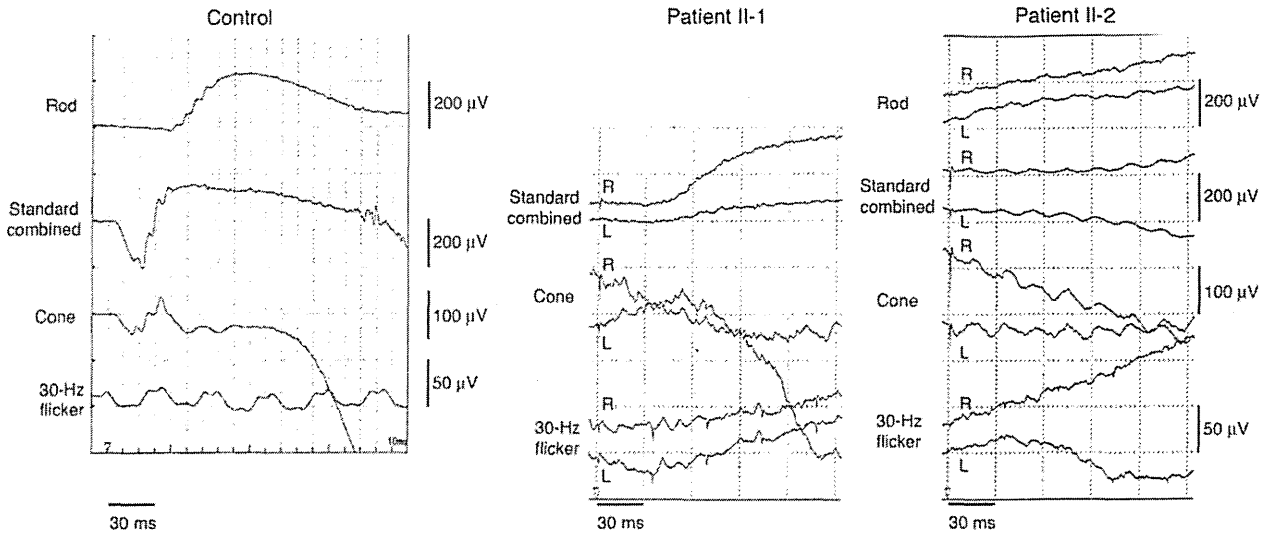

Figure 2. Full-field electroretinogram. The electroretinograms (ERGs; patient II-1) at the age of 9 years, showing no standard combined, photopic, or 30-Hz flicker responses in either eye. The ERGs (patient II-2) at the age of 7 years, showing no rod, standard combined, photopic, or 30-Hz flicker responses in either eye.

Clinical Electrophysiology of Vision. The procedure and conditions for ERG recording have been detailed previously [33].

Fasting venous blood samples were analyzed for glucose, lipid, lipoprotein, and hemogram levels and renal, liver, and thyroid function tests. In addition, hemoglobin A_{1c}, insulin, anti-thyroid peroxidase, anti-thyroglobulin antibodies, cortisol, luteinizing hormone, follicle stimulating hormone, testosterone, estradiol, prolactin, parathyroid hormone, and thyroid receptor antibody levels were examined. Chest X-rays and electrocardiograms were also performed.

DNA preparation and exome sequencing analysis: We obtained venous blood samples from the affected brothers and their unaffected parents. Genomic DNA was extracted from the blood samples by using a Gentra Puregene Blood kit (Qiagen, Tokyo, Japan) and sheared with a Covaris Ultrasonicator (Covaris, Woburn, MA). Construction of paired-end sequence libraries and exome capture were performed by using the Agilent Bravo automated liquid-handling platform with SureSelect XT Human All Exon kit V4 + UTRs kit (Agilent Technologies, Santa Clara, CA) according to the manufacturer's instructions. Enriched libraries were sequenced by using in Illumina HiSeq2000 sequencer (San Diego, CA), according to the manufacturer's instructions for 100-bp paired-end sequencing. Reads were mapped to the reference human genome (1000 genomes phase 2 reference, hs37d5) with Burrows–Wheeler Aligner software version 0.6.2 [34]. Duplicated reads were then removed by Picard MarkDuplicates module version 1.62, and mapped reads around insertion–deletion polymorphisms (INDELs) were realigned by using the Genome Analysis Toolkit (GATK) version 2.1–13 [35]. Base-quality scores were recalibrated by using GATK. Calling of mutations was performed by using the GATK UnifiedGenotyper module, and called single-nucleotide variants and INDELs were annotated by using snpEff software version 3.0 [36]. The mutations were annotated with the snpEff score ("HIGH," "MODERATE," or "LOW") and with the allele frequency in the 1000 genomes database. The mutations were then filtered so that only those with "HIGH" or "MODERATE" snpEff scores (indicating that the amino acid sequence would be functionally affected) and a frequency of less than 1% in the 1000 genome database were analyzed further. We also used new variations, which were not found in the in-house database of seven people exome data with control individuals without ocular diseases. Mutations were classified by hereditary information into homozygous recessive, heterozygous recessive, and de novo mutations in the family members. Filtered mutations were scored with PolyPhen software version 2.2.2 [37], which predicts the effect on the structure and function of the protein. The above exome analysis pipeline is available at Cell Innovation.

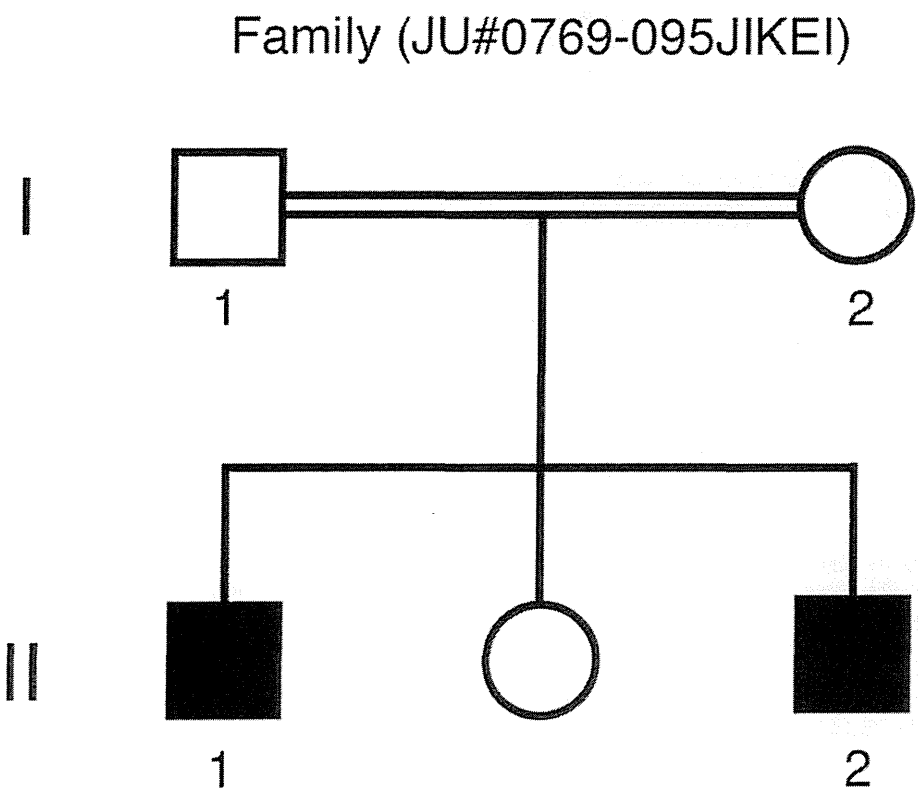

Figure 1. A consanguineous family (JU#0769–095JIKEI) with Alström syndrome. Two affected brothers (II-1 and II-2) with Alström syndrome and their unaffected parents are depicted.

show progressive retinal degeneration, with 90% becoming totally blind by the age of 16 years [19] and all becoming blind eventually [14,19]. Due to severe retinal degeneration and visual impairment during the first months of life, AS is often confused with congenital retinal degenerations, such as Leber congenital amaurosis (LCA) and congenital achromatopsia (ACHM) [20,21]. There are several reports of Japanese patients with AS [22–24]; however, there has been no report identifying any *ALMS1* mutation associated with AS in the Japanese population.

Recently, the development of next-generation sequencing technology has facilitated biologic and biochemical research by enabling the broad analysis of genomes [25–28]. The whole genome of an individual can now be sequenced at great depth, and genomic capture technology can be used to isolate sequences of interest [29–32].

Here, we used whole-exome sequencing to identify a novel *ALMS1* mutation in two Japanese brothers with AS. We also examined the clinical features of the two brothers in detail.

METHODS

The protocol of this study was approved by the Institutional Review Board of the Jikei University School of Medicine and National Hospital Organization Tokyo Medical Center. The protocol adhered to the tenets of the Declaration of Helsinki, and written informed consent was obtained from all participants.

Clinical studies: The study was conducted in one consanguineous Japanese family (JU#0769–095JIKEI) with AS (Figure 1). The parents were second cousins. The clinical history was taken in detail, and the following ophthalmic examinations were performed: decimal best-corrected visual acuity (BCVA), slit-lamp and fundus examinations, and time-domain optical coherence tomography (TD-OCT; OCT3 Stratus; Carl Zeiss Meditec AG, Dublin, CA) or spectral-domain OCT (SD-OCT; Cirrus HD-OCT; Carl Zeiss Meditec AG). In color-vision tests, we used the Ishihara test (38-plate edition) and the Farnsworth Panel D-15 (Panel D-15). Visual-field testing by kinetic perimetry was conducted by using the Goldmann perimeter (GP; Haag Streit, Bern, Switzerland). Full-field electroretinography (ERG) was performed according to the protocols of the International Society for

Molecular Vision 2013; 19:2393-2406 <http://www.molvis.org/molvis/v19/2393>
Received 11 September 2013 | Accepted 22 November 2013 | Published 24 November 2013

Whole-exome sequencing identifies a novel *ALMS1* mutation (p.Q2051X) in two Japanese brothers with Alström syndrome

Satoshi Katagiri,[1,2] Kazutoshi Yoshitake,[3] Masakazu Akahori,[1] Takaaki Hayashi,[2] Masaaki Furuno,[4] Jo Nishino,[3] Kazuho Ikeo,[3] Hiroshi Tsuneoka,[2] Takeshi Iwata[1]

[1]Division of Molecular and Cellular Biology, National Institute of Sensory Organs, National Hospital Organization Tokyo Medical Center, Tokyo, Japan; [2]Department of Ophthalmology, The Jikei University School of Medicine, Tokyo, Japan; [3]Laboratory of DNA Data Analysis, National Institute of Genetics, Shizuoka, Japan; [4]RIKEN Center for Life Science Technologies, Division of Genomic Technologies, Life Science Accelerator Technology Group, Transcriptome Technology Team, Yokohama, Japan

Purpose: No mutations associated with Alström syndrome (AS), a rare autosomal recessive disease, have been reported in the Japanese population. The purpose of this study was to investigate the genetic and clinical features of two brothers with AS in a consanguineous Japanese family.

Methods: Whole-exome sequencing analysis was performed on two brothers with AS and their unaffected parents. We performed a complete ophthalmic examination, including decimal best-corrected visual acuity, slit-lamp and funduscopic examination, visual-field and color-vision testing, full-field electroretinography, and optical coherence tomography. Fasting blood tests and systemic examinations were also performed.

Results: A novel mutation (c.6151C>T in exon 8) in the Alström syndrome 1 (*ALMS1*) gene that causes a premature termination codon at amino acid 2051 (p.Q2051X), was identified in the homozygous state in the affected brothers and in the heterozygous state in the parents. The ophthalmologic findings for both brothers revealed infantile-onset severe retinal degeneration and visual impairment, marked macular thinning, and severe cataracts. Systemic findings showed hepatic dysfunction, hyperlipidemia, hypogonadism, short stature, and wide feet in both brothers, whereas hearing loss, renal failure, abnormal digits, history of developmental delay, scoliosis, hypertension, and alopecia were not observed in either brother. The older brother exhibited type 2 diabetic mellitus and obesity, whereas the younger brother had hyperinsulinemia and subclinical hypothyroidism.

Conclusions: A novel *ALMS1* mutation was identified by using whole-exome sequencing analysis, which is useful not only to identify a disease causing mutation but also to exclude other gene mutations. Although characteristic ophthalmologic findings and most systemic findings were similar between the brothers, the brothers differed slightly in terms of glucose tolerance and thyroid function.

Alström syndrome (AS; OMIM: 203800) is a rare and autosomal recessive hereditary disease with an estimated prevalence of less than 0.001% [1,2]. AS is caused by mutations in the *ALMS1* gene, which is located on chromosome 2p13 [3,4]. ALMS1 is localized to centrosomes and ciliary basal bodies [5,6] and has been implicated in the function, formation, and maintenance of primary cilia [5,7–9]. Dysfunction of primary cilia caused by mutations in genes such as *ALMS1* leads to a multitude of human monogenic disorders known as ciliopathies [10,11]; these include plural systemic diseases, such as AS, Usher syndrome, Bardet–Biedl syndrome (BBS), Senior–Løken syndrome, Joubert syndrome, Meckel–Gruber syndrome, and orofaciodigital syndrome 1 [11,12]. The majority of *ALMS1* mutations are nonsense and frameshift variations (primarily clustered in exons 8, 10, and 16) that are predicted to cause truncated proteins [3,4,13]. In the photoreceptors, *ALMS1* mutations lead to defective function of the connecting cilium.

AS is characterized by a wide spectrum of disorders, such as early onset severe retinal degeneration, obesity from childhood, hyperinsulinemia, type 2 diabetic mellitus (T2DM), hepatic dysfunction, heart failure, sensory hearing loss, and renal failure [14]. Other manifestations include acanthosis nigricans, alopecia, hypogonadism, hypothyroidism, hyperlipidemia, short stature, and scoliosis [15,16]. In most cases of AS, cone–rod degeneration in the first decade, normal intelligence, and no polydactyly serve as a differential diagnosis of BBS, which exhibits similar clinical findings to AS [17].

Almost all patients with AS show nystagmus and severe photophobia from infancy [14,18]. Visual impairment is usually seen at an age younger than 1 year [18]. Although the rate of progression of vision loss is variable, all patients

Correspondence to: Takaaki Hayashi, Department of Ophthalmology, The Jikei University School of Medicine, 3-25-8, Nishi-shimbashi, Minato-ku, Tokyo, 105-8461, Japan; Phone: +81-3-3433-1111 (ext. 3581); FAX: +81-3-5378-8828; email: taka@jikei.ac.jp

11. Szlyk JP, Fishman GA, Alexander KR, Peachey NS, Derlacki DJ (1993) Clinical subtypes of cone–rod dystrophy. Arch Ophthalmol 111:781–788
12. Allikmets R, Singh N, Sun H, Shroyer NF, Hutchinson A, Chidambaram A, Gerrard B, Baird L, Stauffer D, Peiffer A, Rattner A, Smallwood P, Li Y, Anderson KL, Lewis RA, Nathans J, Leppert M, Dean M, Lupski JR (1997) A photoreceptor cell-specific ATP-binding transporter gene (ABCR) is mutated in recessive Stargardt macular dystrophy. Nat Genet 15:236–246
13. Klevering BJ, Yzer S, Rohrschneider K, Zonneveld M, Allikmets R, van den Born LI, Maugeri A, Hoyng CB, Cremers FP (2004) Microarray-based mutation analysis of the *ABCA4* (*ABCR*) gene in autosomal recessive cone–rod dystrophy and retinitis pigmentosa. Eur J Hum Genet 12:1024–1032
14. Klevering BJ, Deutman AF, Maugeri A, Cremers FP, Hoyng CB (2005) The spectrum of retinal phenotypes caused by mutations in the *ABCA4* gene. Graefes Arch Clin Exp Ophthalmol 243:90–100
15. Bayes M, Goldaracena B, Martinez-Mir A, Iragui-Madoz MI, Solans T, Chivelet P, Bussaglia E, Ramos-Arroyo MA, Baiget M, Vilageliu L, Balcells S, Gonzalez-Duarte R, Grinberg D (1998) A new autosomal recessive retinitis pigmentosa locus maps on chromosome 2q31–q33. J Med Genet 35:141–145
16. Tuson M, Marfany G, Gonzalez-Duarte R (2004) Mutation of *CERKL*, a novel human ceramide kinase gene, causes autosomal recessive retinitis pigmentosa (RP26). Am J Hum Genet 74:128–138
17. Auslender N, Sharon D, Abbasi AH, Garzozi HJ, Banin E, Ben-Yosef T (2007) A common founder mutation of *CERKL* underlies autosomal recessive retinal degeneration with early macular involvement among Yemenite Jews. Invest Ophthalmol Vis Sci 48:5431–5438
18. Ali M, Ramprasad VL, Soumittra N, Mohamed MD, Jafri H, Rashid Y, Danciger M, McKibbin M, Kumaramanickavel G, Inglehearn CF (2008) A missense mutation in the nuclear localization signal sequence of CERKL (p.R106S) causes autosomal recessive retinal degeneration. Mol Vis 14:1960–1964
19. Estrada-Cuzcano A, Neveling K, Kohl S, Banin E, Rotenstreich Y, Sharon D, Falik-Zaccai TC, Hipp S, Roepman R, Wissinger B, Letteboer SJ, Mans DA, Blokland EA, Kwint MP, Gijsen SJ, van Huet RA, Collin RW, Scheffer H, Veltman JA, Zrenner E, den Hollander AI, Klevering BJ, Cremers FP (2012) Mutations in *C8orf37*, encoding a ciliary protein, are associated with autosomal-recessive retinal dystrophies with early macular involvement. Am J Hum Genet 90:102–109
20. van Huet RA, Estrada-Cuzcano A, Banin E, Rotenstreich Y, Hipp S, Kohl S, Hoyng CB, den Hollander AI, Collin RW, Klevering BJ (2013) Clinical characteristics of rod and cone photoreceptor dystrophies in patients with mutations in the *C8orf37* gene. Invest Ophthalmol Vis Sci 54:4683–4690
21. Vekslin S, Ben-Yosef T (2010) Spatiotemporal expression pattern of ceramide kinase-like in the mouse retina. Mol Vis 16:2539–2549

Whole-exome sequencing analysis disclosed that our patient had the *EYS* mutations, which demonstrates that the *EYS* mutations can be responsible for both the arCRD and the arRP phenotypes. Interestingly, mutations in the *ABCA4* [12–14], *CERKL* [15–18], and *C8orf37* [19, 20] genes have also been reported to be disease-causing mutations of both the arCRD and arRP phenotypes. With regard to the *ABCA4* gene mutations, the degree of functional damage caused by the various *ABCA4* mutation types can underlie the different degeneration patterns, for example, Stargardt disease (a type of macular dystrophy), arCRD or arRP [12–14]. The majority of patients with *CERKL* mutations exhibit arCRD [17, 18] and less frequently arRP [15, 16]. This is consistent with the fact that the CERKL protein is predominantly expressed in the cone photoreceptors [21]. In addition, different *C8orf37* mutations can cause either the arCRD or arRP phenotypes, which is consistent with the fact that the C8orf37 protein is expressed in both the rod and cone photoreceptors [19, 20]. However, this does not explain the pattern of the photoreceptor degeneration. On the other hand, the compound heterozygous *EYS* mutations (p.Y2935X and p.S1653KfsX2) that were found in our patient have also been reported in an arRP patient [7]. Although it is not understood why the same compound heterozygous mutations would underlie either the arCRD or arRP phenotypes, this finding suggests there is the presence of different modifier alleles between the arCRD or arRP patients with the compound heterozygous *EYS* mutations. Even so, our whole-exome sequencing analysis did not demonstrate any compound heterozygous or homozygous mutations in other 206 retinal disease-associated genes published in the RetNet database.

In conclusion, we demonstrated that *EYS* mutations are the cause of not only arRP but also arCRD. Further investigations will need to be undertaken in order to clarify the prevalence of *EYS* mutations among arCRD patients, and to determine the genotype–phenotype correlations between the arCRD and *EYS* mutations.

Acknowledgments This study was supported by grants to T.I. from the Ministry of Health, Labor and Welfare of Japan (13803661), to M.A. and T.H. from the Ministry of Education, Culture, Sports, Science and Technology of Japan (Grant-in-Aid for Scientific Research C, 25462744 and 25462738), and to T.H. from the Vehicle Racing Commemorative Foundation.

Conflict of interest The authors declare there are no conflicts of interest for this study.

References

1. Abd El-Aziz MM, Barragan I, O'Driscoll CA, Goodstadt L, Prigmore E, Borrego S, Mena M, Pieras JI, El-Ashry MF, Safieh LA, Shah A, Cheetham ME, Carter NP, Chakarova C, Ponting CP, Bhattacharya SS, Antinolo G (2008) *EYS*, encoding an ortholog of Drosophila spacemaker, is mutated in autosomal recessive retinitis pigmentosa. Nat Genet 40:1285–1287
2. Collin RW, Littink KW, Klevering BJ, van den Born LI, Koenekoop RK, Zonneveld MN, Blokland EA, Strom TM, Hoyng CB, den Hollander AI, Cremers FP (2008) Identification of a 2 Mb human ortholog of Drosophila eyes shut/spacemaker that is mutated in patients with retinitis pigmentosa. Am J Hum Genet 83:594–603
3. Abd El-Aziz MM, O'Driscoll CA, Kaye RS, Barragan I, El-Ashry MF, Borrego S, Antinolo G, Pang CP, Webster AR, Bhattacharya SS (2010) Identification of novel mutations in the ortholog of Drosophila eyes shut gene (*EYS*) causing autosomal recessive retinitis pigmentosa. Invest Ophthalmol Vis Sci 51:4266–4272
4. Audo I, Sahel JA, Mohand-Said S, Lancelot ME, Antonio A, Moskova-Doumanova V, Nandrot EF, Doumanov J, Barragan I, Antinolo G, Bhattacharya SS, Zeitz C (2010) *EYS* is a major gene for rod-cone dystrophies in France. Hum Mutat 31:E1406–E1435
5. Bandah-Rozenfeld D, Littink KW, Ben-Yosef T, Strom TM, Chowers I, Collin RW, den Hollander AI, van den Born LI, Zonneveld MN, Merin S, Banin E, Cremers FP, Sharon D (2010) Novel null mutations in the *EYS* gene are a frequent cause of autosomal recessive retinitis pigmentosa in the Israeli population. Invest Ophthalmol Vis Sci 51:4387–4394
6. Hosono K, Ishigami C, Takahashi M, Park DH, Hirami Y, Nakanishi H, Ueno S, Yokoi T, Hikoya A, Fujita T, Zhao Y, Nishina S, Shin JP, Kim IT, Yamamoto S, Azuma N, Terasaki H, Sato M, Kondo M, Minoshima S, Hotta Y (2012) Two novel mutations in the *EYS* gene are possible major causes of autosomal recessive retinitis pigmentosa in the Japanese population. PLoS ONE 7:e31036
7. Iwanami M, Oshikawa M, Nishida T, Nakadomari S, Kato S (2012) High prevalence of mutations in the *EYS* gene in Japanese patients with autosomal recessive retinitis pigmentosa. Invest Ophthalmol Vis Sci 53:1033–1040
8. Hayashi T, Gekka T, Kozaki K, Ohkuma Y, Tanaka I, Yamada H, Tsuneoka H (2012) Autosomal dominant occult macular dystrophy with an *RP1L1* mutation (R45W). Optom Vis Sci 89:684–691
9. Katagiri S, Yoshitake K, Akahori M, Hayashi T, Furuno M, Nishino J, Ikeo K, Tsuneoka H, Iwata T (2013) Whole-exome sequencing identifies a novel *ALMS1* mutation (p.Q2051X) in two Japanese brothers with Alström syndrome. Mol Vis 19:2393–2406
10. Yagasaki K, Jacobson SG (1989) Cone–rod dystrophy. Phenotypic diversity by retinal function testing. Arch Ophthalmol 107:701–708

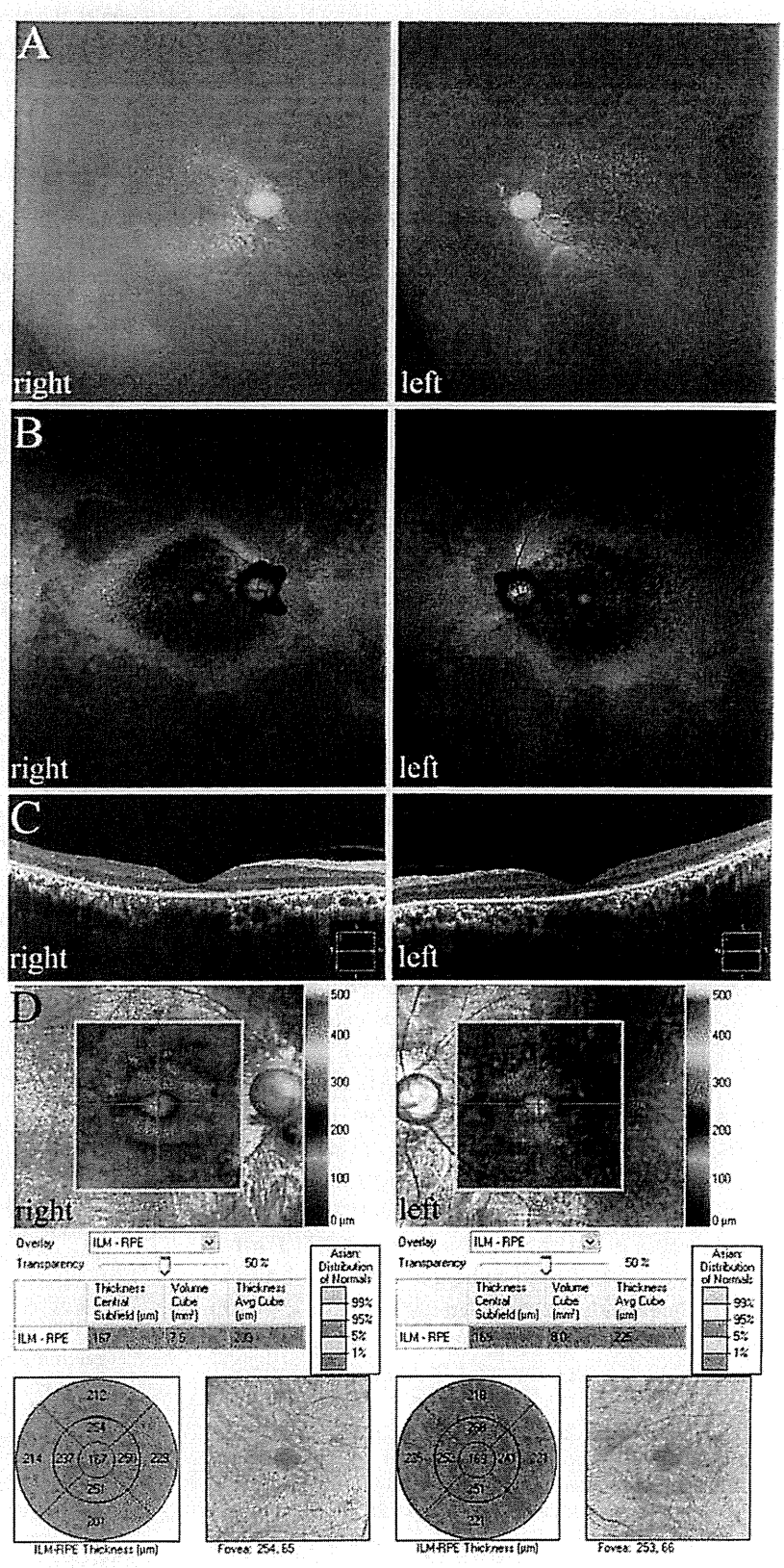

Fig. 5 Fundus photographs, fundus autofluorescence images (FAI), and optic coherence tomography images (OCT) at the age of 36 years. **a** Fundus photographs show retinal degenerations within the vascular arcades in both eyes, but relatively preserved mid-peripheral to peripheral retinal findings with no apparent attenuation of the retinal vessels. **b** FAI shows decreased autofluorescence within the vascular arcades but increased autofluorescence of the foveal area, and increased autofluorescence outside the vascular arcades in both eyes. **c** OCT (HD 5-line raster scan) shows retinal thinning with a visible foveal external limiting membrane line in both eyes. **d** OCT (Macular cube scan) shows entire macular thinning in both eyes

Molecular Vision 2013; 19:1580-1590 <http://www.molvis.org/molvis/v19/1580>
Received 1 April 2013 | Accepted 15 July 2013 | Published 20 July 2013

Molecular characteristics of four Japanese cases with *KCNV2* retinopathy: Report of novel disease-causing variants

Kaoru Fujinami,[1,2] Kazushige Tsunoda,[1] Natsuko Nakamura,[1] Yu Kato,[1] Toru Noda,[1] Kei Shinoda,[3] Kaoru Tomita,[4] Tetsuhisa Hatase,[5] Tomoaki Usui,[6] Masakazu Akahori,[1] Takeshi Itabashi,[1] Takeshi Iwata,[1] Yoko Ozawa,[2] Kazuo Tsubota,[2] Yozo Miyake[1,7]

[1]National Institute of Sensory Organs, National Tokyo Medical Center, Tokyo, Japan; [2]Department of Ophthalmology, Keio University, School of Medicine, Tokyo, Japan; [3]School of Medicine, Teikyo University, Tokyo, Japan; [4]Heiwa Ganka Clinic, Tokyo, Japan; [5]Graduate School of Medical and Dental Sciences, Niigata University, Niigata, Japan; [6]Akiba Eye Clinic, Niigata, Japan; [7]Aichi Medical University, Aichi, Japan

Purpose: To describe the molecular characteristics of four Japanese patients with cone dystrophy with supernormal rod responses (CDSRR).

Methods: Four individuals with a clinical and electrophysiological diagnosis of CDSRR were ascertained. The pathognomonic findings of the full-field electroretinograms (ERGs) included a decrease in the rod responses, a square-shaped a-wave, an excessive increase in the b-wave in the bright flash responses, and decreased cone-derived responses. Mutational screening of the coding regions and flanking intronic sequences of the potassium channel, subfamily V, member 2 (*KCNV2*) gene was performed with bidirectional sequencing. The segregation of each allele was confirmed by screening other family members. Subsequent in silico analyses of the mutational consequences for protein function were performed.

Results: There were two siblings from one family and one case in each of the two families. One family had a consanguineous marriage. Mutational screening revealed compound heterozygosity for the two alleles, p.C177R and p.G461R, in three patients, and homozygosity for complex alleles, p.R27H and p.R206P, in one patient from the consanguineous family. There were three putative novel variants, p.R27H, p.C177R, and p.R206P. The four variants in the families with *KCNV2* were highly conserved in other species. In silico analyses predicted that all of the missense variants would alter protein function.

Conclusions: Biallelic disease-causing variants were identified in four Japanese patients with CDSRR suggesting that the pathognomonic electrophysiological features are helpful in making a molecular diagnosis of *KCNV2*. Three novel variants were identified, and we conclude that there may be a distinct spectrum of *KCNV2* alleles in the Japanese population.

Patients with cone dystrophy and supernormal rod electroretinograms (ERGs) were first reported in 1983, and the abnormality in the ERGs indicated a progressive degeneration of the cone photoreceptors associated with unique rod system abnormalities [1]. More detailed characteristics of this rare, autosomal recessive condition were reported in later studies, and the disease was named cone dystrophy with supernormal rod responses (CDSRR; MIM #610356) [2-8].

Most cases with CDSRR typically present in the first two decades of life with reduced visual acuity, abnormal color vision, and photophobia [8-11]. Night blindness is a later feature of the disorder [8]. The fundus appearance is variable, with some having a normal peripheral retina and a range of macular abnormalities [8-10]. The pattern of the autofluorescence (AF) images is also variable: Young cases have either a normal pattern or small parafoveal ring enhancements, while older cases have a narrow high-signal annulus that can encircle a central atrophic area of the retinal pigment epithelium (RPE) [6,12]. Recently, spectral domain optical coherence tomography (SD-OCT) and adaptive optics scanning laser ophthalmoscope (AOSLO) studies have described morphological changes of the fovea even at the early stages [10,13,14].

The electrophysiological findings are pathognomonic of CDSRR, and they assist in its early diagnosis [3,5,8-12,15-17]. The light-adapted ERGs are usually delayed and decreased in keeping with a generalized cone system dysfunction. There is also a unique rod system abnormality; the dark-adapted ERGs elicited by dim flashes are markedly decreased and delayed, and increasing the flash intensity results in an excessive increase in the b-wave amplitude accompanied by a shortening of the peak time of the b-wave [8,9,11]. A square-shaped a-wave trough of the dark-adapted bright flash ERGs is also a characteristic feature of this disorder [9,11].

Correspondence to: Kazushige Tsunoda, Laboratory of Visual Physiology, National Institute of Sensory Organs, 2-5-1 Higashigaoka, Meguro-ku, Tokyo 152-8902, Japan; Phone: +81334110111; FAX: +81334110185; email: tsunodakazushige@kankakuki.go.jp

CDSRR has been shown to be caused by mutations in the potassium channel, subfamily V, member 2 (*KCNV2*) gene (MIM# 607,604), which encodes a voltage-gated potassium channel subunit, Kv8.2 [18]. This silent subunit is expressed in rod and cone photoreceptors [18-20], and is thought to assemble with other K^+ channel subunits such as KCNB1, KCNC1, and KCNF1. These subunits form functional heteromeric channels with altered properties that have a narrowed membrane potential for activation and slow inactivation kinetics [19]. Eventually, these kinetic properties result in transient hyperpolarization overshoots on rapid changes in the inward currents [19]. A deficiency of Kv8.2 by a mutation in *KCNV2* may affect the characteristics of the I_{ks} as first described in amphibian photoreceptors [21]. This deficiency may influence the photoreceptor membrane potential. However, the underlying mechanisms that fully explain the clinical features of CDSRR are still not determined.

More than 50 different disease-causing variants in *KCNV2* have been reported: small insertion and deletion changes or large deletions that constitute a protein truncation and single nucleotide changes with amino acid substitutions [9,10,13,14,16,18,22,23]. Three small case series describe the clinical features of CDSRR in East Asians [3,5,15]; however, molecular genetic studies of these populations have not been published. Thus, the purpose of this study was to determine the molecular genetic characteristics from the clinical and electrophysiological findings of four Japanese patients who were diagnosed with CDSRR.

METHODS

Subjects: Four subjects who were diagnosed with CDSRR from the clinical and electrophysiological findings were ascertained at the National Institute of Sensory Organs, National Tokyo Medical Center, Tokyo, Japan and Niigata University, Niigata, Japan. The natural history of these four patients has been partially reported recently [24]. The procedures used were approved by the ethics committee of each institution, and all procedures were performed in accordance with the principles of the Declaration of Helsinki. Informed consent was obtained from all experimental subjects for all procedures.

Clinical assessment: A complete medical history was obtained, and a comprehensive ophthalmological examination was performed on all patients. The photophobia and night blindness episode was obtained on direct questioning. The clinical assessments included measurements of the best-corrected visual acuity (BCVA), dilated ophthalmoscopy, color fundus photography, AF imaging, OCT, and electrophysiological recordings. AF images were obtained with the HRA 2 confocal scanning laser ophthalmoscope (Heidelberg Engineering, Heidelberg, Germany; excitation light, 488 nm; barrier filter, 500 nm; field of view, 30×30°) [25]. The OCT images were obtained with SD-OCT (Cirrus HD-OCT, versions 4.5 and 5.1; Carl Zeiss Meditec, Dublin, CA) [26].

Electrophysiological assessments: Full-field ERGs were recorded from the four patients with the minimum standard protocol of the International Society for Clinical Electrophysiology of Vision (ISCEV) [27]. The ERG examination included the following: (i) dark adapted dim flash 0.01 $cd \cdot s \cdot m^{-2}$ (DA 0.01), (ii) dark adapted bright flash 30.0 $cd \cdot s \cdot m^{-2}$ (DA 30.0), (iii) light adapted 3.0 $cd \cdot s \cdot m^{-2}$ at 2 Hz (LA 3.0), and (iv) light adapted 3.0 $cd \cdot s \cdot m^{-2}$ 30 Hz flicker ERG (LA 3.0 30Hz). The extended protocol included the recording of the dark-adapted ERGs elicited by stimulus intensities of 0.001 $cd \cdot s \cdot m^{-2}$, 0.01 $cd \cdot s \cdot m^{-2}$, 0.3 $cd \cdot s \cdot m^{-2}$, 3.0 $cd \cdot s \cdot m^{-2}$, and 30.0 $cd \cdot s \cdot m^{-2}$. Two of the four patients were also recorded with the extended protocol. An excessive or disproportionate increase in the dark adapted b-wave with increasing flash intensity was assessed in these two patients, according to the previous report [9].

Mutational screening: After informed consent was obtained, blood samples were collected in EDTA tubes from each subject, and the DNA was extracted with a DNA extraction kit (QIAamp DNA Blood Maxi Kit; Qiagen, Venlo, the Netherlands). All exons and exon–intron boundaries were amplified with polymerase chain reaction (PCR), and the primer sequences used are shown in Table 1. PCR was performed with 20 µl volume containing 0.5 Unit Taq polymerase (PrimeStar GXL DNA polymerase, Takara, Tokyo, Japan). The sequence was determined based on the dideoxy terminator method using an ABI PRISM 3100×l Genetic Analyzer (Applied Biosystems, Foster City, CA) according to the manufacturer's protocol. The SeqScape Software version 2.5 (Applied Biosystems) was used to analyze the sequence alignment. Bidirectional Sanger sequencing was also performed in other family members of the proband, to confirm the segregation of the alleles.

Molecular genetic analyses: All of the missense variants identified were analyzed using two software prediction programs, Sorting Intolerant from Tolerance (SIFT) and PolyPhen2 [28,29]. The predicted effects on splicing of all missense variants were assessed with the Human Splicing finder program version 2.4.1. The allele frequency of each variant was estimated with the Exome Variant Server (NHLBI Exome Sequencing Project, Seattle, WA). A multiple sequence alignment program for DNA or proteins, the Clustal Omega, was applied to confirm an evolutionary conservation. Likely non-disease-causing variants (polymorphisms)

Table 1. Primer Sequences and Conditions for *KCNV2* Mutational Screening.

Primer	Sequence (5'–3')	Product size (bp)	PCR annealing (°C)
E1aF	AGGACCTGAGAAGGGGCAGCT	831	71
E1aR	TCCAGGAGGCGGAGGAACTCT		
E1bF	CCCTGCTGTCCACGCTGAATG	799	71
E1bR	CAGCGTGGGTAAGGTGGGTCA		
E1cF	AAGATCCAGCACGAGCTGCGC	841	65
E1cR	ATGGATGTCAAAAGTGGTGGA		
E2aF	AGCTTCTGTTCTTTTCATGAC	624	63
E2aR	GTCTCATAGTTGCTCTGTGTT		

bp = base pairs.

were also analyzed with the same protocol applied to likely disease-causing variants.

RESULTS

The demographic features of the four individuals from three families with CDSRR are summarized in Table 2. There were two siblings (patients 1 and 2) in one family and one case in each of the two families (patients 3 and 4). The pedigree of each family is shown in Figure 1, and a consanguineous marriage was present in family 3.

Clinical findings: The age of the patient at the time of the examination was 23, 17, 21, and 17 years with the age of disease onset at 9, 5, 3, and 2 years (Table 2). Three patients complained of photophobia (patients 1, 2, and 4), and all four patients had night blindness. Patient 4 had had mild nystagmus since age 2 years. The decimal BCVA of the four patients ranged from 0.08 to 0.8, and the BCVA of patients 1 and 2 was better than 0.7 in each eye.

The findings obtained from the color fundus photographs, AF images, and SD-OCT images are summarized in Figure 1 and Table 2. The fundus photographs showed mottling of the RPE at the macula in all four patients with subtle patchy granular flecks at the macula in patient 3. A ring enhancement of the AF signal was detected in the AF images of all four patients; three subjects had it centered on the fovea (patients 1, 2, and 3), and one had it at the parafovea (patient 4). In patient 3, the ring enhancement at the fovea was surrounded by patchy granular foci of the high AF signal at the macula.

SD-OCT demonstrated abnormalities in the outer retinal layers in all four patients. The cone outer segment tip line was absent in the macular area in all patients. The photoreceptor inner and outer segment junction line was discontinuous at the fovea in patients 3 and 4, and thinning of the outer retina was detected at the fovea in all four patients.

Electrophysiological assessments: The electrophysiological findings are summarized in Table 3, and the ERGs are shown in Figure 2. The full-field ERGs were recorded with the minimum ISCEV standard from patients 2 and 3, and extended protocol full-field ERGs including the dark-adapted ERGs elicited by an intensity series were obtained from patients 1 and 4.

The dark adapted b-wave amplitude elicited by a stimulus intensity 0.01 (DA0.01) was delayed and decreased in patients 3 and 4, but was normal but delayed in patient 1. The responses for DA0.01 were undetectable in patient 2. An excessive increase in the b-wave for the extended protocol was found in two patients, 1 and 4. In addition, the a-wave was square-shaped with a supernormal b-wave elicited by stimulus intensity 30.0 (DA 30.0) in all four patients. The photopic ERGs (LA 3.0 and LA 3.0 30Hz) were decreased in all four patients (Table 3 and Figure 2).

Molecular genetics: The molecular genetic findings are summarized in Table 2 and Appendix 1. Likely disease-causing variants in *KCNV2* were identified in all four patients. The four likely disease-causing variants were p.Arg27His, p.Cys177Arg, p.Arg206Pro, and p.Gly461Arg (Appendix 1), and two likely non-disease-causing variants (polymorphisms) were p.Gly61Gly and p.Ala265Ala (Appendix 2). The segregation of each allele was confirmed by screening of other family members for all these variants.

Detailed molecular results including in silico analysis to assist in predicting the pathogenicity of the four disease-causing variants identified are shown in Appendix 1. All of the four likely disease-causing variants were single nucleotide changes with one amino acid substitution (missense), i.e., p.Arg27His, p.Cys177Arg, p.Arg206Pro, and p.Gly461Arg. Compound heterozygosity for the two alleles, p.Cys177Arg and p.Gly461Arg, in patients 1, 2, and 3 and homozygosity for the complex alleles, p.Arg27His and p.Arg206Pro, in patient

Table 2. Summary of demographics, clinical findings and molecular status for four Japanese patients with *KCNV2*-retinopathy

Pt, FM, gender	Onset of disease, age at examination (years)	VA		Fundus		AF		OCT		Mutation status
		RE	LE	RPE mottling	Subtle patchy granular flecks	Ring enhancement	Patchy granular foci of high signal	Absence of COST	Deficit of IS/OS	
1, 1, F	9, 23	0.7	0.8	Macula	ND	Fovea	ND	Fovea	ND	Compund heterozygous [c.529 T>C, p.Cys177Arg]; [c.1381G>A, p.Gly461Arg]
2, 1, M	5,17	0.7	0.7	Macula	ND	Fovea	ND	Fovea	ND	Compund heterozygous [c.529 T>C, p.Cys177Arg]; [c.1381G>A, p.Gly461Arg]
3, 2, F	3,21	0.1	0.1	Macula	Macula	Fovea	Macuala	Macula	Fovea	Compund heterozygous [c.529 T>C, p.Cys177Arg]; [c.1381G>A, p.Gly461Arg]
4, 3, F	2, 17	0.1	0.08	Macula	ND	Para-fovea	ND	Macula	Fovea	Complex homozygous [c.80 G>A, p.Arg27His]; [c.617 G>C, p.Arg206Pro]

Pt = Patient; FM = family number; VA = logMAR visual acuity; RE = right eye; LE = left eye; RPE = retinal pigment epithelium; AF = autofluorescence; COST = cone outer segment tip line; IS/OS = photoreceptor inner and outer segment junction; ND = not detected. The affected area of each finding is based on the color fundus photographs, AF images, and the OCT images in each column.

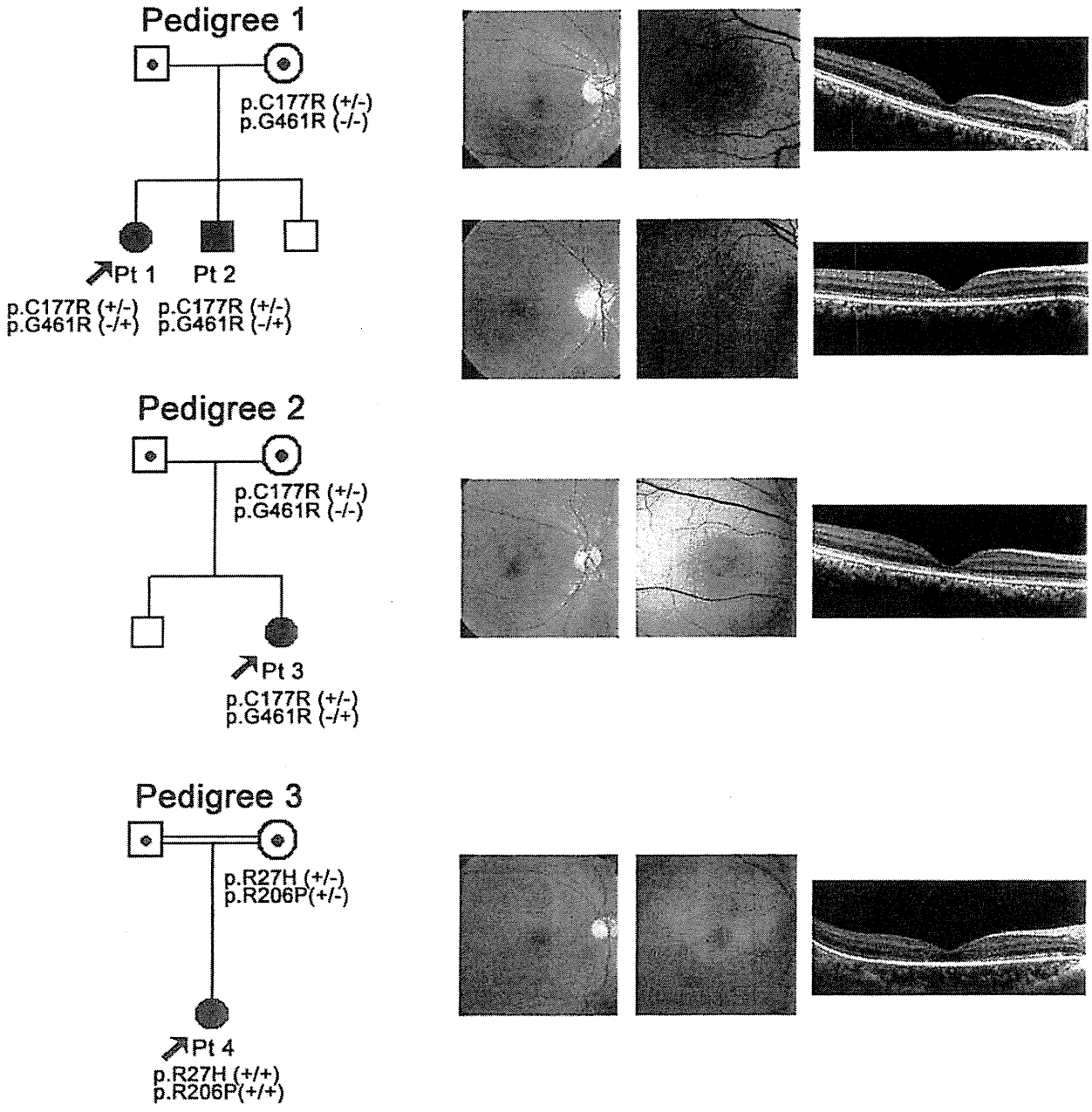

Figure 1. Pedigree and retinal imaging of each patient with potassium channel, subfamily V, member 2 retinopathy. Pedigrees with molecular status of the three families with potassium channel, subfamily V, member 2 (*KCNV2*) retinopathy are shown on the left. Retinal images including color fundus photographs, autofluorescence images, and spectral domain optical coherence tomography are presented on the right. Images of patient 1 (top row), patient 2 (second row from top), patient 3 (third row from top), and patient 4 (bottom row) are shown.

4 were revealed by the segregation analyses. The p.Gly461Arg variant has been reported, and the p.Arg27His, p.Cys177Arg, and p.Arg206Pro variants are putative novel. In silico analysis revealed an "intolerant" protein function or a "probably or possibly damaged" protein but no effect on splicing in the three putative novel variants (SIFT, Poplyphen2, and Human Splicing finder; Appendix 1). The reported missense variant, p.Gly461Arg, with possibly affecting splicing was detected in six out of 13,006 individuals of the Exome Variant Server; the three novel variants, p.Arg27His, p.Cys177Arg, and

Molecular Vision 2013; 19:1580-1590 <http://www.molvis.org/molvis/v19/1580>
© 2013 Molecular Vision

Table 3. Electrophysiological Findings of Four Japanese Patients with KCNV2-retionpathy

Pt	DA 0.01		DA 30.0				Square shaped a-wave	Excessive enlargement of b-wave in the extended protocol	LA 3.0			LA 3.0 30Hz		
			A-wave		B-wave				A-wave	B-wave		B-wave		
	Amp (μv)	PT (ms)	Amp	PT	Amp	PT			Amp	PT	Amp	PT	Amp	PT
1	N	Del	N	Del	Super N	NA	(+)	(+)	Sub N	Del	Sub N	UD	UD	UD
2	UD	UD	N	Del	Super N	NA	(+)	NA	Sub N	Del	Sub N	Del	Sub N	Del
3	Sub N	Del	N	Del	Super N	N	(+)	NA	Sub N	Del	Sub N	Del	Sub N	N
4	Sub N	Del	N	Del	Super N	NA	(+)	(+)	Sub N	Del	Sub N	Del	Sub N	Del

Pt = patient; Amp = amplitude; PT = peak time; N = normal; UD = undetectable response; Sub N = subnormal; Del = delayed response; Super N=supernormal response; NA = not available. Full-field electroretinography (ERG) incorporating the standards of the International Society for Clinical Electrophysiology of Vision (ISCEV) included: (i) dark adapted dim flash 0.01 cd•s•m^{-2} (DA0.01), (ii) dark adapted bright flash 30.0 cd•s•m^{-2} (DA30.0), (iii) light adapted 3.0 cd•s•m^{-2} at 2 Hz (LA 3.0), and (iv) light adapted 3.0 cd•s•m^{-2} 30 Hz flicker (LA 3.0 30 Hz). The extended protocol also included the recording of dark adapted responses to an intensity series of flashes in order to detect an excessive enlargement of dark adapted b-wave (patients 1 and 4).

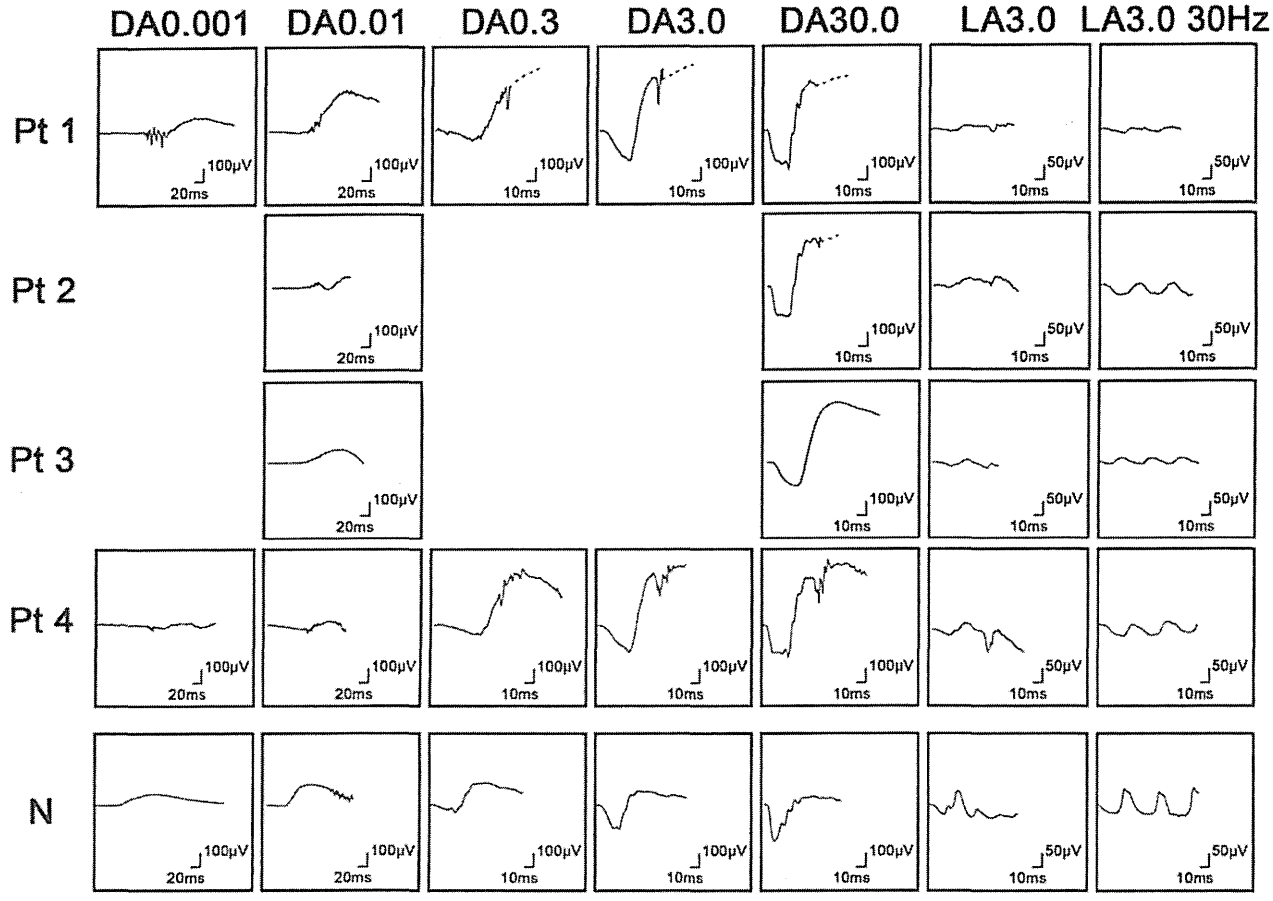

Figure 2. Electrophysiological findings of each patient with potassium channel, subfamily V, member 2 (*KCNV2*) retinopathy. Full-field electroretinograms (ERGs) of patient 1 (top row), patient 2 (second row), patient 3 (third row), and patient 4 (forth row) are shown. The ERGs from a normal control (bottom row) are also shown for comparison. All four patients underwent full-field ERG testing with the minimum standards of the International Society for Clinical Electrophysiology of Vision (ISCEV): (i) dark adapted dim flash 0.01 cd•s•m^{-2} (DA 0.01), (ii) dark adapted bright flash 30.0 cd•s•m^{-2} (DA 30.0), (iii) light adapted 3.0 cd•s•m^{-2} at 2 Hz (LA 3.0), and (iv) light adapted 3.0 cd•s•m^{-2} 30 Hz flicker ERG (LA 3.0 30Hz). The extended protocol was applied to two subjects (patients 1 and 4), including the recording of dark-adapted ERGs to an intensity series of flashes; 0.001 cd•s•m-^{2}, 0.01 cd•s•m^{-2}, 0.3 cd•s•m^{-2}, 3.0 cd•s•m^{-2}, and 30.0 cd•s•m^{-2}.

p.Arg206Pro, were not identified. Three missense variants, p.Arg27His, p.Cys177Arg, and p.Arg206Pro, were highly conserved among the orthologs, and one missense variant, p.Gly461Arg, was completely conserved (Figure 3).

A model of the *KCNV2* protein structure showing the approximate position of the missense disease-causing variants identified is presented in Figure 4. The KCNV2 protein comprises 545 amino acids and contains an N-terminal A and B box (NAB) and six transmembrane domains, (S1–S6), with a K selective motif, GlyTyrGly, in the pore-forming loop (P loop) between S5 and S6 [18]. One variant is located within the N-terminus (p.Arg27His), two variants, p.Cys177Arg and p.Arg206Pro, within the NAB, and one variant, p.Gly461Arg, within the P-loop.

Detailed molecular results of two non-disease-causing variants (polymorphisms) including the in silico analyses are summarized in Appendix 2. These two homozygous variants, p.Gly61Gly and p.Ala265Ala, were synonymous changes in the cording region and were predicted to be benign or have no effect on splicing (Polyphen2 and Human Splicing finder program analysis). Both were present in a high number of chromosomes in the Exome Variant Server database (7647/13006 for p.Gly61Gly and 5636/13006 for p.Ala265Ala, respectively).

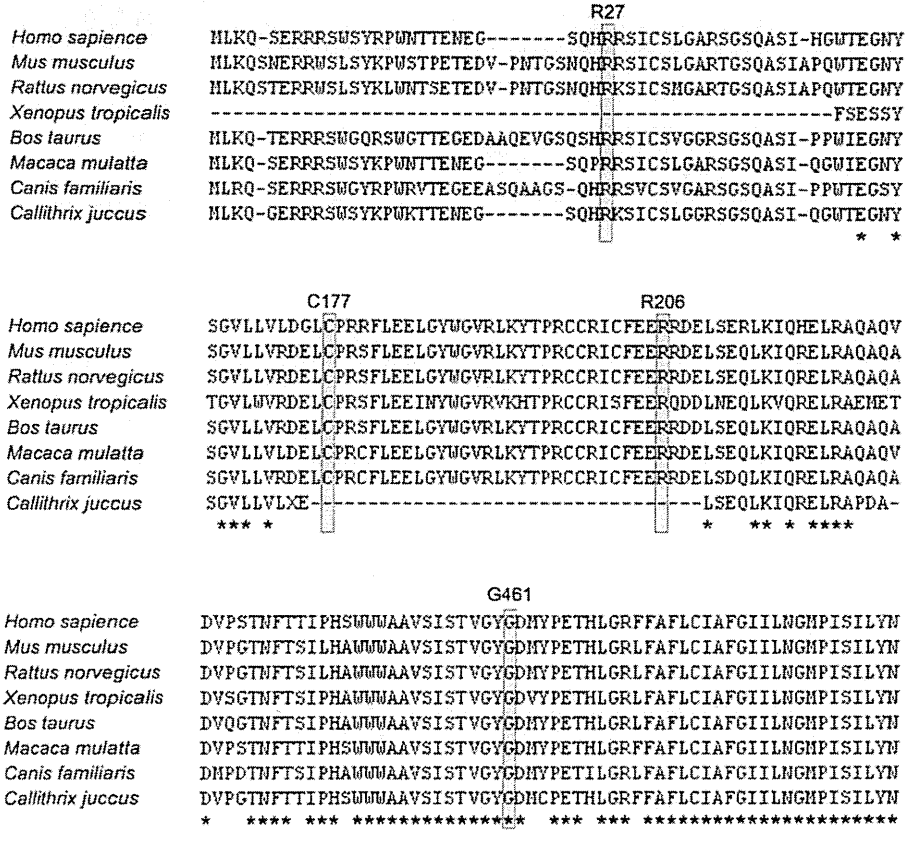

Figure 3. Multiple alignment of eight species of potassium channel, subfamily V, member 2 orthologs. The amino acid-sequence alignment is numbered in accordance with the *Homo sapiens* potassium channel, subfamily V, member 2 (*KCNV2*) sequence (ENSP00000371514). The positions of mutated residues, Arg27 (c.80 G>A, p.Arg27His), Arg177 (c.529 T>C, p.Cys177Arg), Arg206 (c.617 G>C, p.Arg206Pro), and Gly461 (c.1381 G>A, p.Gly461Arg), are highlighted. The alignment was performed with the Clustal Omega program, and the asterisk indicates a completely conserved residue.

DISCUSSION

Our results showed the molecular genetic characteristics of four Japanese patients with CDSRR, which, to the best of our knowledge, is the first report of these characteristics of *KCNV2* retinopathy in an East Asian population. Our four patients harbored the likely disease-causing variants in *KCNV2*. Compound heterozygosity for two alleles, p.Cys177Arg and p.Gly461Arg, in three patients and homozygosity for two complex alleles, p.Arg27His and p.Arg206Pro, in one subject were confirmed. Three of the four variants, p.Arg27His, p.Cys177Arg, and p.Arg206Pro, were novel, which indicates all genotypes identified in our series have never been described before.

The clinical and electrophysiological characteristics of our four patients were similar to those of reported patients [8-11,13,14,17,18]. Additionally, all four patients presented with a decrease in central vision whose onset was in the first decade of life with minimal fundus changes and a characteristic ring enhancement of the AF signal (Table 2 and Figure 1). These findings are also in accordance with earlier reports [9-12,14]. SD-OCT demonstrated a discontinuous or absent inner and outer segment junction line in two patients

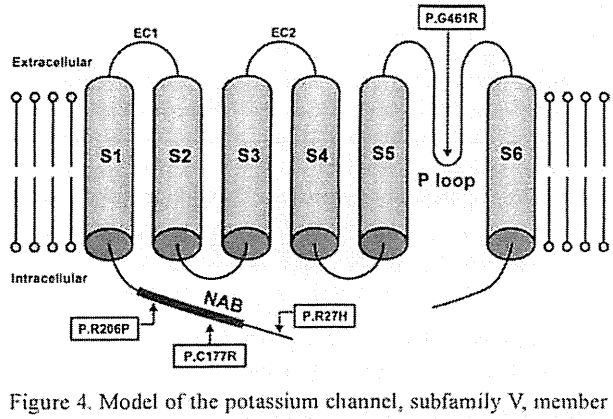

Figure 4. Model of the potassium channel, subfamily V, member 2 protein structure. A schematic representation of the potassium channel, subfamily V, member 2 (*KCNV2*) subunit of the K channel is drawn showing the approximate position of missense disease-causing variants identified in this study. The *KCNV2* protein consists of an N-terminus, an N-terminal A and B box (NAB), and six transmembrane domains (S1–S6), with two extracellular loops (EC 1, 2) and a K selective motif, GlyTyrGly, in the pore-forming loop (P loop) between S5 and S6.

as previously reported [10]. In addition, the absence of the cone outer segment tip line at the macular region was also confirmed in all four patients.

The pathognomonic electrophysiological features were demonstrated in all four patients, viz., delayed and reduced photopic ERGs, delayed ERGs for DA 0.01, and a square-shaped a-wave with a supernormal b-wave for DA 30.0 (Table 3 and Figure 2). An excessive increase in the b-wave for the DA ERGs to an intensity series of flashes was also confirmed in patients 2 and 3. Therefore, the unique rod system abnormalities were identical to those reported for *KCNV2* retinopathy [9,14].

Compound heterozygosity for two alleles, p.Cys177Arg and p.Gly461Arg, was found in patients 1, 2, and 3. The p.Gly461Arg with relatively higher allele frequency affects the third residue of the ultraconserved-GYG-tripeptide motif that acts as an ion selectivity filter in the K channel's pore-forming loop, P loop, between S5 and S6 (Figure 4) [30]. The clinical effect of p.Gly461Arg was well characterized earlier [10,16,17]. Friedburg et al. reported that three siblings with homozygous p.Gly461Arg had a relatively severe phenotype with an early onset and nystagmus at <5 years of age, visual acuity decrease (0.1–0.25, constantly), minimal fundus changes, ring enhancement at the foveal AF image, and an excessive increase in the b-wave for scotopic ERGs to an intensity series [17]. In contrast to the previous reports on homozygous patients, the three patients with heterozygous p.Gly461Arg in our series did not have nystagmus, and two of our patients had less severe BCVA decrease (0.7–0.8). These findings imply that the phenotype of the compound heterozygous for p.Gly461Arg and p Cys177Arg could have a less severe phenotype than those homozygous for p.Gly461Arg. It is of interest that the phenotypic spectrum, compound heterozygous for p.Gly461Arg and p Cys177Arg, was also observed in our series. Two relatively mild phenotypes were observed in the two siblings in our series (patients 1 and 2). In addition, one relatively severe phenotype, with more severe visual acuity decrease (0.1) and photoreceptor/RPE abnormalities at the macula, was detected in patient 3.

Three of the new disease-causing missense variants were located within the N-terminal region of the protein (Figure 4): p.Arg27His within the N-terminus and p.Cys177Arg and p.Arg206Pro within NAB. p.Cys177Arg was completely segregated, and the predicted pathogenesis and evolutionary conservation were confirmed. The coexistence of two likely disease-causing variants, p.Arg27His and p.Arg206Pro, on the same chromosome was also identified in our series with segregation analyses. The patient who was homozygous for these two complex variants had a severe phenotype, with an early onset (2 years), nystagmus, and severe visual acuity decrease (0.1 to 0.08). Both variants were predicted to be pathogenic with evolutionary high conservation (Appendix 1and Figure 3). Whether one of these variants is a neutral polymorphisms in cis with disease-causing one, or whether family 4's alleles are complex with two independently damaging missense variants remains to be determined.

To conclude, this study further delineates the molecular genetic findings of *KCNV2* retinopathy. Three putative novel variants were identified in our four Japanese patients with CDSRR, and our findings suggest there may be a distinct spectrum of *KCNV2* alleles in the Japanese population. However, the clinical findings were similar to that of the reported other population. Electrophysiology was fundamental to the diagnosis with pathognomonic findings due to channelopathy. The pathognomonic characteristics may be a useful method of determining the success of clinical therapeutic trials with gene replacement or pharmacological treatments for channelopathy.

APPENDIX 1. RESULTS OF IN SILICO MOLECULAR GENETIC ANALYSIS OF *KCNV2* MUTATIONS IDENTIFIED.

To access the data, click or select the words "Appendix 1." Pt = patient; Hom = homozygous; Het = heterozygous; SIFT = sorting Intolerant from Tolerance; HSF = human splicing finder program; CV = consensus values; EVS = exome variant server; POD = possibly damaging; PRD = probably damaging; ND = not detected. SIFT (version 4.0.4) results are reported to be tolerant if tolerance index ≥ 0.05 or intolerant if tolerance index < 0.05. Polyphen-2 (vision 2.1) appraises mutations qualitatively as Benign, Possibly Damaging or Probably Damaging based on the model's false positive rate. The cDNA is numbered according to Ensemble transcript ID ENST00000382082, in which +1 is the A of the translation start codon. Human splicing finder version 2.4.1 was applied to predict the effect of each variant on splicing. The results from HSF matrix indicate the values for the wild type and mutant sequences. The larger difference of values between the wild type and the mutant sequences indicates the greater change that the variant can affect on the splice site. EVS denotes variants in the Exome Variant Server, NHLBI Exome Sequencing Project, Seattle, WA.

APPENDIX 2. MOLECULAR ANALYSIS OF *KCNV2* POLYMORPHISMS.

To access the data, click or select the words "Appendix 2." Pt = patient; Hom = homozygous; Het = heterozygous; SIFT = sorting Intolerant from Tolerance; HSF = human splicing

finder program; CV = consensus values; EVS = exome variant server.

ACKNOWLEDGMENTS

We are grateful to the patients who kindly agreed to take part in this study and colleagues who referred individuals to us at National Institute of Sensory Organs. We thank Professor Duco I. Hamasaki (Bascom Palmer Eye Institute, Miami, FL) for proofreading. This research is supported in part by research grants from the Ministry of Health, Labor and Welfare, Japan and Grant-in-Aid for Scientific Research from JSPS.

REFERENCES

1. Gouras P, Eggers HM, MacKay CJ. Cone dystrophy, nyctalopia, and supernormal rod responses. A new retinal degeneration. Arch Ophthalmol 1983; 101:718-24. [PMID: 6601944].
2. Alexander KR, Fishman GA. Supernormal scotopic ERG in cone dystrophy. Br J Ophthalmol 1984; 68:69-78. [PMID: 6607068].
3. Yagasaki K, Miyake Y, Litao RE, Ichikawa K. Two cases of retinal degeneration with an unusual form of electroretinogram. Doc Ophthalmol 1986; 63:73-82. [PMID: 3015524].
4. Foerster MH, Kellner U, Wessing A. Cone dystrophy and supernormal dark-adapted b-waves in the electroretinogram. Graefes Arch Clin Exp Ophthalmol 1990; 228:116-9. [PMID: 2186970].
5. Kato M, Kobayashi R, Watanabe I. Cone dysfunction and supernormal scotopic electroretinogram with a high-intensity stimulus. A report of three cases. Doc Ophthalmol 1993; 84:71-81. [PMID: 8223112].
6. Rosenberg T, Simonsen SE. Retinal cone dysfunction of supernormal rod ERG type. Five new cases. Acta Ophthalmol (Copenh) 1993; 71:246-55. [PMID: 8333273].
7. Hood DC, Cideciyan AV, Halevy DA, Jacobson SG. Sites of disease action in a retinal dystrophy with supernormal and delayed rod electroretinogram b-waves. Vision Res 1996; 36:889-901. [PMID: 8736222].
8. Michaelides M, Holder GE, Webster AR, Hunt DM, Bird AC, Fitzke FW, Mollon JD, Moore AT. A detailed phenotypic study of "cone dystrophy with supernormal rod ERG". Br J Ophthalmol 2005; 89:332-9. [PMID: 15722315].
9. Robson AG, Webster AR, Michaelides M, Downes SM, Cowing JA, Hunt DM, Moore AT, Holder GE. "Cone Dystrophy with Supernormal Rod Electroretinogram": A Comprehensive Genotype/Phenotype Study Including Fundus Autofluorescence and Extensive Electrophysiology. Retina 2010; 30:51-62. [PMID: 19952985].
10. Sergouniotis PI, Holder GE, Robson AG, Michaelides M, Webster AR, Moore AT. High-resolution optical coherence tomography imaging in KCNV2 retinopathy. Br J Ophthalmol 2012; 96:213-7. [PMID: 21558291].
11. Vincent A, Robson AG, Holder GE. PATHOGNOMONIC (DIAGNOSTIC) ERGs A Review and Update. Retina 2013; 33:5-12. [PMID: 23263253].
12. Khan AO, Alrashed M, Alkuraya FS. 'Cone dystrophy with supranormal rod response' in children. Br J Ophthalmol 2012; 96:422-6. [PMID: 21900228].
13. Zobor D, Kohl S, Wissinger B, Zrenner E, Jagle H. Rod and Cone Function in Patients with KCNV2 Retinopathy. PLoS ONE 2012; 7:e46762-[PMID: 23077521].
14. Vincent A, Wright T, Garcia-Sanchez Y, Kisilak M, Campbell M, Westall C, Heon E. Phenotypic Characteristics including in vivo Cone Photoreceptor Mosaic in KCNV2-Related 'Cone Dystrophy with Supernormal Rod Electroretinogram'. Invest Ophthalmol Vis Sci 2013; 30:898-908. .
15. Tanimoto N, Usui T, Ichibe M, Takagi M, Hasegawa S, Abe H. PIII and derived PII analysis in a patient with retinal dysfunction with supernormal scotopic ERG. Doc Ophthalmol 2005; 110:219-26. [PMID: 16328930].
16. Wissinger B, Dangel S, Jagle H, Hansen L, Baumann B, Rudolph G, Wolf C, Bonin M, Koeppen K, Ladewig T, Kohl S, Zrenner E, Rosenberg T. Cone dystrophy with supernormal rod response is strictly associated with mutations in KCNV2. Invest Ophthalmol Vis Sci 2008; 49:751-7. [PMID: 18235024].
17. Friedburg C, Wissinger B, Schambeck M, Bonin M, Kohl S, Lorenz B. Long-term follow-up of the human phenotype in three siblings with cone dystrophy associated with a homozygous p.G461R mutation of KCNV2. Invest Ophthalmol Vis Sci 2011; 52:8621-9. [PMID: 21911584].
18. Wu H, Cowing JA, Michaelides M, Wilkie SE, Jeffery G, Jenkins SA, Mester V, Bird AC, Robson AG, Holder GE, Moore AT, Hunt DM, Webster AR. Mutations in the gene KCNV2 encoding a voltage-gated potassium channel subunit cause "cone dystrophy with supernormal rod electroretinogram" in humans. Am J Hum Genet 2006; 79:574-9. [PMID: 16909397].
19. Czirják G, Toth ZE, Enyedi P. Characterization of the heteromeric potassium channel formed by kv2.1 and the retinal subunit kv8.2 in Xenopus oocytes. J Neurophysiol 2007; 98:1213-22. [PMID: 17652418].
20. Hölter P, Kunst S, Wolloscheck T, Kelleher DK, Stieht C, Wolfrum U, Spessert R. The retinal clock drives the expression of Kcnv2, a channel essential for visual function and cone survival. Invest Ophthalmol Vis Sci 2012; 53:6947-54. [PMID: 22969075].
21. Beech DJ, Barnes S. Characterization of a voltage-gated K+ channel that accelerates the rod response to dim light. Neuron 1989; 3:573-81. [PMID: 2642011].
22. Thiagalingam S, McGee TL, Weleber RG, Sandberg MA, Trzupek KM, Berson EL, Dryja TP. Novel mutations in the KCNV2 gene in patients with cone dystrophy and a supernormal rod electroretinogram. Ophthalmic Genet 2007; 28:135-42. [PMID: 17896311].

23. Wissinger B, Schaich S, Baumann B, Bonin M, Jagle H, Friedburg C, Varsanyi B, Hoyng CB, Dollfus H, Heckenlively JR, Rosenberg T, Rudolph G, Kellner U, Salati R, Plomp A, De Baere E, Andrassi-Darida M, Sauer A, Wolf C, Zobor D, Bernd A, Leroy BP, Enyedi P, Cremers FP, Lorenz B, Zrenner E, Kohl S. Large deletions of the KCNV2 gene are common in patients with cone dystrophy with supernormal rod response. Hum Mutat 2011; 32:1398-406. [PMID: 21882291].

24. Nakamura N, Tsunoda K, Fujinami K, Shinoda K, Tomita K, Hatase T, Usui T, Akahori M, Iwata T, Miyake Y. Long-term Observation over Ten Years of Four Cases of Cone Dystrophy with Super-normal Rod Electroretinogram . Nippon Ganka Gakkai Zasshi 2013; In press.

25. Fujinami K, Tsunoda K, Hanazono G, Shinoda K, Ohde H, Miyake Y. Fundus autofluorescence in autosomal dominant occult macular dystrophy. Arch Ophthalmol 2011; 129:597-602. [PMID: 21555613].

26. Tsunoda K, Usui T, Hatase T, Yamai S, Fujinami K, Hanazono G, Shinoda K, Ohde H, Akahori M, Iwata T, Miyake Y. Clinical characteristics of occult macular dystrophy in family with mutation of RpIII gene. Retina 2012; 32:1135-47. [PMID: 22466457].

27. Marmor MF, Fulton AB, Holder GE, Miyake Y, Brigell M, Bach M. ISCEV Standard for full-field clinical electroretinography (2008 update). Doc Ophthalmol 2009; 118:69-77. [PMID: 19030905].

28. Ng PC, Henikoff S. SIFT: Predicting amino acid changes that affect protein function. Nucleic Acids Res 2003; 31:3812-4. [PMID: 12824425].

29. Adzhubei IA, Schmidt S, Peshkin L, Ramensky VE, Gerasimova A, Bork P, Kondrashov AS, Sunyaev SR. A method and server for predicting damaging missense mutations. Nat Methods 2010; 7:248-9. [PMID: 20354512].

30. Heginbotham L, Lu Z, Abramson T, MacKinnon R. Mutations in the K+ channel signature sequence. Biophys J 1994; 66:1061-7. [PMID: 8038378].

Articles are provided courtesy of Emory University and the Zhongshan Ophthalmic Center, Sun Yat-sen University, P.R. China. The print version of this article was created on 20 July 2013. This reflects all typographical corrections and errata to the article through that date. Details of any changes may be found in the online version of the article.

Clinical Ophthalmology

Dovepress

CASE REPORT

Two siblings with late-onset cone–rod dystrophy and no visible macular degeneration

Hiroyuki Sakuramoto[1]
Kazuki Kuniyoshi[1]
Kazushige Tsunoda[2]
Masakazu Akahori[2]
Takeshi Iwata[2]
Yoshikazu Shimomura[1]

[1]Department of Ophthalmology, Kinki University Faculty of Medicine, Osaka-Sayama City, Osaka, Japan; [2]National Institute of Sensory Organs, National Hospital Organization Tokyo Medical Center, Tokyo, Japan

Background: We report our findings in two siblings with late-onset cone–rod dystrophy (CRD) with no visible macular degeneration.

Cases and methods: Case 1 was an 82-year-old man who first noticed a decrease in vision and color blindness in his early seventies. His mother and younger sister also had visual disturbances. His decimal visual acuity was 0.3 in the right eye and 0.2 in the left eye. Ophthalmoscopy showed normal fundi, and fluorescein angiography was also normal in both eyes. The photopic single flash and flicker eletroretinograms (ERGs) were severely attenuated and the scotopic ERGs were slightly reduced in both eyes. Case 2 was the 80-year-old younger sister of Case 1. She first noticed a decline in vision and photophobia in both eyes in her early seventies. Her decimal visual acuity was 0.4 in the right eye and 0.2 in the left eye. Ophthalmoscopy showed mottling of the retinal pigment epithelium in the midperiphery with no visible macular degeneration. The photopic single flash and flicker ERGs were severely attenuated, and the scotopic ERGs were slightly reduced in both eyes.

Conclusion: These siblings are the oldest reported cases of CRD with no visible macular degeneration. Thus, CRD should be considered in patients with reduced visual acuity, color blindness, and photophobia even if they are older than 70 years.

Keywords: cone–rod dystrophy, peripheral cone dystrophy, occult macular dystrophy, late onset, macular degeneration, negative ERG

Introduction

Cone–rod dystrophy (CRD) is an inherited retinal dystrophy that is characterized by reduced visual acuity, color blindness, and photophobia.[1–3] The age of onset generally ranges from the teens to the thirties,[2,3] and most patients with CRD have atrophic macular degeneration with a bull's eye lesion, or midperipheral degeneration in the late stages of the disease.[2,3] Patients with CRD can also have a central scotoma, and constriction of the peripheral visual fields at the end stages of the disease.[2,3] The cone-driven electroretinograms (ERGs) are attenuated even in the early stages, and this reduction is essential for making a diagnosis of CRD.[2,3]

Cases of atypical CRD, such as CRD with normal fundi,[4–7] occult macular dystrophy (OMD; Miyake disease),[8–11] peripheral cone dystrophy,[12–15] fundus albipunctatus associated with cone dystrophy,[16,17] and cone dystrophy with supernormal rod ERGs[18,19] have also been reported.

We present the clinical features of two siblings with CRD who had only mild fundus abnormalities. Their mother was also known to have visual difficulties, but was already dead at the time the two siblings were examined.

Correspondence: Kazuki Kuniyoshi
Department of Ophthalmology, Kinki University Faculty of Medicine, 377-2 Ohno-Higashi, Osaka-Sayama City, Osaka 589-8511, Japan
Tel +81 723 660 221
Fax +81 723 682 559
Email kazuki@med.kindai.ac.jp